Simulation of superconducting quantum circuits

Author: Pau Fargas Reixats[†‡]
Facultat de Física, Universitat de Barcelona, Diagonal 645, 08028 Barcelona, Spain[†]
Qilimanjaro Quantum Tech, 08007, Barcelona, Spain[‡]

Advisors: Albert Solana[‡] & Bruno Juliá[†]

Abstract: We present a simulation of a transmon qubit, one of the most used charge qubits in quantum computing. The relevance of such a device comes from its low noise sensitivity compared to other superconducting qubits. The aim of the simulation is to describe the energy spectrum and explain the behaviour of the noise sensitivity. This work is framed in a bigger simulator and it consists of the first step of the full transmon simulator: a backend simulator with the capability to control a general superconducting chip architecture with external microwave pulses.

I. INTRODUCTION

Quantum computation and information have the potential to revolutionize modern computing by enabling exponential speedups for certain types of problems [1]. Among the most promising avenues for realizing such computation lies in superconducting quantum circuits, which find their foundation in Josephson junctions (Ref.[2], section 4.6).

The initial challenge is to find a suitable system to develop a chip. To be able to control the chip, energy levels must be distinguishable, that is, the energy difference between two consecutive energy levels i and j, ΔE_{ij}, cannot be equal to any other: $\Delta E_{ij} \neq \Delta E_{kl}$ such that $kl \neq ij, ji$. The main example of such a system is the atom: its energy levels are not equally spaced through the entire spectrum. Those devices that can reproduce the energy levels and other atom characteristics, like selection rules, are called *artificial atoms*, and they bring some advantages over the natural atom, like for instance, parameter tunability [3].

Even though there are many different technologies (Ref.[2], section 1 and Table 6.1), superconducting circuits are a notable option when talking about speed and control, but suffer from large external noise sensitivity.

The superconducting technology aims to create a solid-state device that can behave as an artificial atom. This can be achieved thanks to the Josephson effect, a quantum effect that occurs when two superconductors are separated by a thin insulating barrier, leading to a probability of tunnelling for the Cooper pairs of electrons. This tunnelling creates a non-linear effect which leads to an induced anharmonicity, i.e. energy levels without equally spaced gaps. Some examples of superconducting circuits can be found in Ref.[4].

The superconducting circuit that we will use here will be a kind of charge qubit (Figure 1a of Ref. [4]): the *transmon* qubit (Ref.[5]). The transmon qubit is a variation of the CPB (section II D) that has a ratio between the Josephson energy and the charging energy in the order of $\sim 10^2$. If we compare it to the CPB, it has a smaller but enough anharmonicity, while achieving a substantial reduction in charge noise. Transmon qubits have been used to demonstrate a range of crucial quantum computing tasks, such as quantum error correction and quantum simulation.

II. FUNDAMENTAL CONCEPTS

Before conducting a comprehensive analysis of the simulated circuit, it is imperative to clarify certain foundational concepts about the realm of superconductivity and the predecessors of the *transmon*.

A. The LC circuit and the quantum harmonic oscillator

According to [6] the quantum harmonic oscillator (QHO) is a system whose Hamiltonian is given by:

$$\hat{H} = \frac{\hat{p}^2}{2m} + \frac{1}{2}m\omega^2\hat{x}^2 \tag{1}$$

Where $\hat{p}$ is the momentum operator, m represents the mass, ω is the oscillation frequency and $\hat{x}$ is the position operator. Its energy levels are given by:

$$E_n = \hbar\omega\left(n + \frac{1}{2}\right) \tag{2}$$

Which are equally spaced by $\hbar\omega$. One system that can be described by this Hamiltonian is the LC circuit: A resonant circuit composed of an inductor and a capacitor in series (section 4.4 of Ref.[2]). This system will be the basis for the description of the *transmon qubit*.

B. Cooper pairs, superconductivity and the Josephson effect

Superconductivity is a macroscopic phenomenon in which certain materials exhibit zero electrical resistance and the expulsion of magnetic fields. Currently, it is explained by the BCS theory [7], in which the fundamental concept is the *Cooper pair*:

Cooper pairs are pairs of electrons that form a bound state with zero total momentum due to the interaction with the phonons of the lattice. This bound state is a boson-like quasiparticle, so it can be described with the Bose-einstein statistics, leading to the possibility of a macroscopic occupation of the same quantum state and moving together coherently. This implies that the electrons can move without resistance, thus emerging superconductivity.

This phenomenon needs cryogenic temperatures, because the attractive force between electrons and phonons is very weak, and thermal energy can break the bound state.
Thanks to this phenomenon, an interesting effect occurs in superconductors: The *Josephson effect* is a quantum mechanical effect that takes place in superconductors, where a current flows between two superconductors separated by a thin insulating barrier. This current involves the tunnelling of Cooper pairs of electrons through the insulating barrier.
The *Josephson effect* is desirable because it induces a non-linear term in the Hamiltonian. The physical implementation is what is called a *Josephson Junction*. The physical implementation of the Josephson junction consists of a thin capacitor, with superconducting electrodes, typically made of aluminium, and an insulating barrier made of aluminium oxide. In Figure 1 b) one can see a real image of a Josephson junction. The dimension of this device is in the order of hundreds of nanometers (see Figure 1 b)) [8], [9].

C. Number-phase representation

The number-phase representation is based on section 4.9 of Ref.[2].
Before acting on the systems, the Hilbert space in which the elements work will be defined. Because the elements that are being treated are electrical circuit components, its Hilbert space is constituted by the charge $\hat{q}$ and flux $\hat{\phi}$ variables such that $[\hat{\phi}_b, \hat{q}_{b'}] = i\hbar\delta_{bb'}$.
In this work, it has been used the *number representation*. The number operator is defined as $\hat{q} = -2e\hat{n}$, where e is the electron charge so that $\hat{n}$ expresses the imbalance of Cooper pairs in the junction. In this representation, one can write the charge operator (or the number operator) diagonally, such that $\hat{n} = \sum_n n|n\rangle\langle n|$. Now it is needed to explore the expression of the phase or flux operators in the number basis by looking at the Lie algebra they generate.
Defining the phase operator $\hat{\varphi} = 2\pi\frac{\hat{\phi}}{\Phi_0}$, one can obtain the following relation:

$$e^{i\hat{\varphi}}|n\rangle = |n-1\rangle \tag{3}$$

And the exponential can be written as:

$$e^{i\hat{\varphi}} = \sum_n |n-1\rangle\langle n| \tag{4}$$

From here, one can see that:

$$\cos\hat{\varphi} = \frac{1}{2}\left(\sum_n |n+1\rangle\langle n| + |n\rangle\langle n+1|\right) \tag{5}$$

This last result will be used in future sections.

D. The Cooper pair box

The Cooper pair box (CPB) [10] is a superconducting circuit that consists of a superconducting island connected to a superconducting reservoir by a Josephson junction. The implementation and equivalent circuit are in Figure 1, subfigures *a* and *c*. Its Hamiltonian is given by (section 4.6 Ref.[2]):

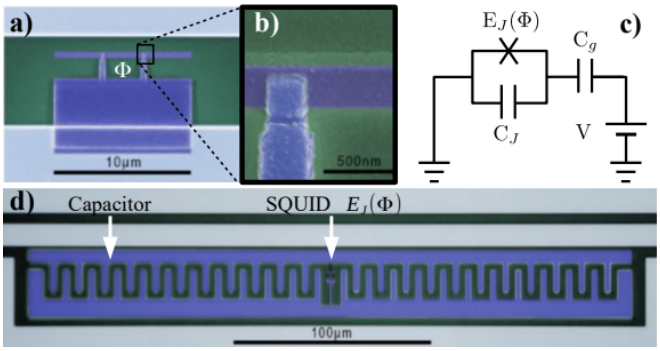

FIG. 1: Figure 6.2 from Ref.[2]. a) Superconducting island coupled to the ground through two Josephson junctions. A Cooper Pair Box b) One junction c) Equivalent circuit of the image. The Josephson junction is represented by a capacity connected in parallel to an ideal Josephson junction (one with no capacity). d) Image of the implementation of a transmon qubit

$$\hat{H} = \frac{1}{2C_\Sigma}(\hat{q} - \hat{q}_g)^2 - E_J\cos(\hat{\varphi}) \tag{6}$$

Where C_Σ is the total capacitance of the circuit, $\hat{q}$ is the charge operator, $\hat{\varphi}$ the superconducting phase, and $\hat{q}_g \equiv -C_g V$ is the offset charge.
We can use the number operator from section II C and the charging energy $E_C = \frac{e^2}{2C}$ we obtain:

$$\hat{H} = 4E_C(\hat{n} - n_g)^2 - E_J\cos(\hat{\varphi}) \tag{7}$$

Something interesting about the last term is that the factor E_J, the Josephson energy, can be tuned externally. This is achieved by substituting the Josephson junction with a *dc-SQUID*. In this context, *SQUID* (section 4.7 of Ref.[2]) stands for *s*uperconducting *qu*antum *i*nterference *d*evice. These kinds of devices are used as high-precise magnetometers in many industries. In the field of superconducting artificial atoms, the *dc-SQUID* is used as an effective Josephson junction that permits tuning its Josephson energy with an external magnetic flux $E_J = E_J(\Phi)$. This work will not account for external time-dependent magnetic fields, so the Josephson energy is supposed to be constant.

III. TRANSMONS

The *transmission-line shunted plasma oscillation*[5] or *transmon* qubit, is related to the CPB in its design, but with the ratio $\frac{E_J}{E_C} \sim 10^2$. As Figure 1 d) shows, his difference is achieved by enlarging the gate capacity C_G, and it leads to an exponential decrease of the charge dispersion, while losing anharmonicity by a weak power law [5].

A. Hamiltonian and analytical solution

Similarly to the CPB, the transmon is built by coupling two superconducting islands by a Josephson junction (Ref.[5], section IIA). Its effective Hamiltonian is the same form as the CPB, in equation 7.
The eigenenergies of the transmon can be found analytically on the basis of the phases. The Hamiltonian is written as:

$$\hat{H} = 4E_C \left(-i\frac{\partial}{\partial\hat{\varphi}} - n_g\right)^2 - E_J\cos(\hat{\varphi}) \tag{8}$$

According to Ref.[11] equation 1.18, Schrödinger's equation of the system with a Hamiltonian with the form of 7 takes the form of a Mathieu equation. The full derivation can be found in Ref.[11], section 1.1.3; Ref.[2], section 6.3.3 and Ref.[5], Appendix B.
The fact that this system has an analytical solution has been used in the comparison of the results obtained in the comparison of Figure 4, as Ref.[5] uses this solution to present its results.

B. QHO vs Transmon: Eigenenergies

An interesting exercise to do is to see how the transmon is different from a QHO in terms of its eigenenergies. To do that, an analytical approximation of the transmon eigenenergies will be used to compare them with the analytical expression of the QHO eigenenergies.
Setting $\hbar = 1$ from the section II A, the energy levels of the QHO are given by:

$$\omega_n = \omega\left(n + \frac{1}{2}\right) \tag{9}$$

Taking the result of section *4. The Quantized Transmon* in [12] for the energy levels of a transmon:

$$\omega_j = \left(\omega - \frac{\delta}{2}\right)j + \frac{\delta}{2}j^2 \tag{10}$$

Where $\delta \equiv -E_C < 0$.
In figure 2, one can see the ground state and the first two excited levels for both circuits.
This approximation shows, in an instructive manner, the significance of superconductivity in the fabrication of artificial atoms: It introduces the non linear term in the energies, leading to an *induced anharmonicity*, i.e. a different energy gap between levels.

IV. NUMERICAL SIMULATIONS

The objective of the simulation was to achieve the matrix form of the Hamiltonian and obtain its eigenvalues by diagonalizing it. To diagonalize the Hamiltonian, the *eigh* function of the *numpy* Python library was used [13]. Then, results will be compared with [5] to check for correctness. Lastly, it is expected to justify why the *transmon* is a significant improvement over earlier superconducting qubits.

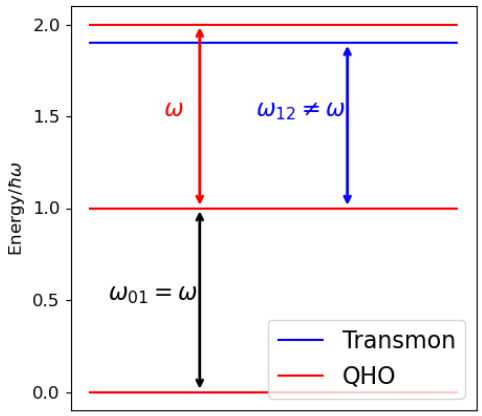

FIG. 2: Energy levels representation of a transmon and a quantum harmonic oscillator, using the expression 10. As one can see, up to the fourth order of magnitude without the fast-rotating terms, the first energy level is the same for both systems, but the second level of the transmon differs from its first gap

A. Matrix representation

The usual way to tackle this problem to simulate this circuit as a qubit, is to use the two-level approximation. In this way, the Hamiltonian of the system is given by [2]:

$$\mathcal{H} = \frac{\hbar\Delta}{2}\hat{\sigma}^z + \frac{\hbar\Omega}{2}\hat{\sigma}^x \tag{11}$$

Where $\hat{\sigma}^z$, $\hat{\sigma}^x$ are the z and x Pauli matrices, $\hbar$ the reduced Plank constant, Δ the qubit gap $\Delta \equiv \hbar\omega_{01} = E_1 - E_0$ and Ω is associated with microwaves that couple the off-diagonal dipolar moment operator and induce transitions between eigenstates.
But in our case, we will use the full lumped-element Hamiltonian (eq. 7). That is because we want to be able to work with not just the first two states, but to check for leakage into other excited states, or even working with qudits, quantum systems with d states.
Making use of the relation 5, we can write the full lumped-element Hamiltonian as follows:

$$\hat{H} = 4E_C(\hat{n} - n_g)^2 - \frac{1}{2}E_J\left(\sum_n |n+1\rangle\langle n| + |n\rangle\langle n+1|\right) \tag{12}$$

Then we can write this expression in its matrix form. In general, we can define:

$$M_{JU} = \sum_n |n+1\rangle\langle n| \quad M_{JL} = \sum_n |n\rangle\langle n+1| \tag{13}$$

$$M_J = M_{JU} + M_{JL} = \sum_n |n+1\rangle\langle n| + |n\rangle\langle n+1| \tag{14}$$

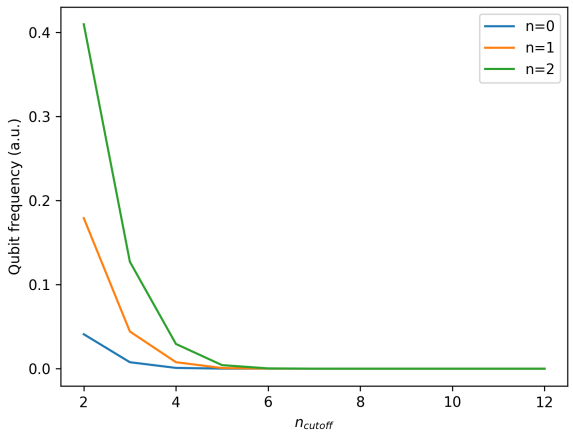

FIG. 3: Convergence of the eigenvalues with the dimension cutoff. The qubit frequency is calculated like $E(n_{cutoff}) - E(n_{cutoff})^{min}$ so that every energy tends to zero. In this way, one can observe the convergence much better for the 3 energy levels at the same time.

So that M_{JU} represents the upper diagonal term, and M_{JL} represents the lower diagonal term. Then M_J is a matrix such that only the upper and lower diagonals are different from zero. Then we can write the Hamiltonian on the charge basis as follows:

$$\hat{H} = 4E_C(\hat{n} - n_g)^2 - \frac{1}{2}E_J M_J \tag{15}$$

This operator is represented by an infinite large matrix, so we truncated it to a cutoff $|n| \leq n_{cutoff} = 10$ reasonable to the problem we want to solve (which in our case is to simulate up to three levels of energy), then the matrix will be of dimension $(2 \cdot n_{cuttof} + 1) \times (2 \cdot n_{cuttof} + 1) = 21 \times 21$. In figure 3 it can be seen the convergence of the eigenvalues with the n_{cutoff} parameter. Then the operator $\hat{n}$ is expressed as:

$$\hat{n} = \sum_{n=-n_{cutoff}}^{n_{cutoff}} n|n\rangle\langle n| \tag{16}$$

B. Transmon simulation

After obtaining the matrix form of the problem, the results will be presented in the following section.
One of the important things to reproduce was the eigenvalues of the Hamiltonian. Figure 4 shows the energy bands along different values of the offset charge n_g, for four different ratios between the two involved energies.
There, one can see that as we approach the transmon regime, the energy bands get flatter, but it can be seen that the gaps between energy levels change too. This could lead to approaching the QHO regime, which is needed to be avoided. To study this phenomenon, one has to define a new magnitude:

$$\alpha \equiv E_{21} - E_{10} \qquad \alpha_r \equiv \frac{\alpha}{E_{01}} \tag{17}$$

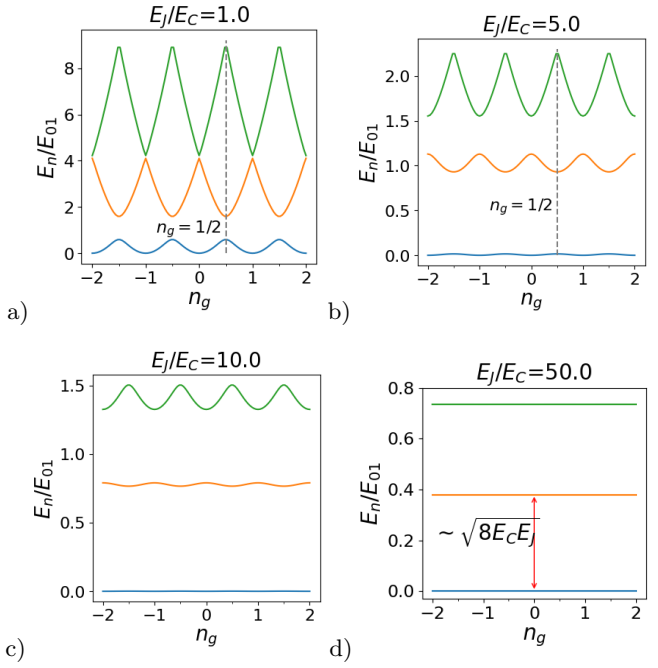

FIG. 4: Plots for four different ratios $\frac{E_J}{E_C}$, showing the energy bands along the effective offset charge n_g. Figure 2 in Ref[5] shows the analytical solution for the eigenenergies. By comparing the shape of the two figures, we conclude our results are correct.

α is called the anharmonicity and α_r is the relative anharmonicity. The dependency of those two new magnitudes is studied in Figure 5

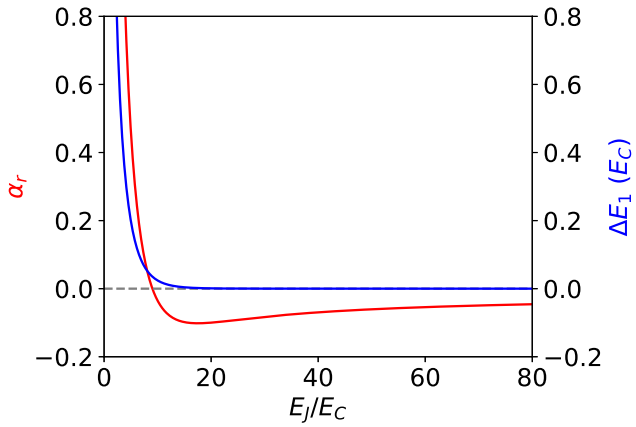

FIG. 5: Relative anharmonicity α_r (red) and charge dispersion for the first excited level ΔE_1(blue) versus E_J/E_C.

As one can infer from the definition of α and α_r, if the value is zero, the system behaves like a QHO. So to see the advantage of this kind of qubit, we have to take a look at its charge dispersion.
The charge dispersion tells how sensitive is the system to external charges, and it is related to the parameter n_g.

It can be defined as:

$$\Delta E_m \equiv E_m(n_g = 0) - E_m(n_g = 1/2) \tag{18}$$

If Figure 4 is inspected, one can see that if n_g changes, the eigenvalues of the qubit do too. But as the ratio E_J/E_C is increased, the energy bands tend to be flat, meaning that the charge offset, which is related to the charge sensitivity, becomes irrelevant. This property makes the transmon insensitive to charge noise. In Figure 5, one can see that the correlation between that ratio and the charge dispersion decays as an exponential function.
It can be observed that the charge dispersion tends to zero much faster than the relative anharmonicity. In Ref.[5] it is shown analytically that the charge dispersion is given by an exponential decrease (equation 2.5) while the anharmonicity loss tends to zero with a weak power-law (equation 2.12).

V. CONCLUSIONS

This work has focused on explaining one kind of charge qubit, the *transmon* qubit: an improvement of its predecessor, the *Cooper Pair Box*.
It has been shown that the transmon improves the charge dispersion of the qubit, increasing its dephasing time T_2 (Ref.[5], section V), while maintaining sufficient anharmonicity to operate as a qubit.
Although the Hamiltonian that represents the transmon has an analytical solution ([5],[2] section 6.3.3), this work is justified as a baseline of a more general simulator, consisting of a time-dependent term and couplings, which will be used as the way to control the qubit to perform operations. In the scope of this project, the evolution of the single transmon time-dependent Hamiltonian with an external pulse and a coupling with a microwave resonating cavity was discussed, but the integrator used to solve the von Neumann equation never converged. After some investigation, it was found that we were not taking into account the different effects that occur when coupling to an electromagnetic field, such as the Stark effect or the Lamb shift of the frequency.

Other milestones achieved in the project were the development of an abstract class that outputs the full-time-independent Hamiltonian of an arbitrary configuration of transmons and resonating cavities, taking into account interactions between transmons and resonating cavities. This part of the project helped me understand how chip architecture is thought of and why is that it is nearly impossible to have a fully connected chip. Because of space restrictions, the theory and the results obtained are not presented.

This work is just a small glimpse into the larger problem of what can be done with this kind of simulation. The next steps for this project would be to implement the time dependency with an external pulse by tuning the frequency at which one has to send the pulse, for one single transmon coupled to a resonator cavity and the pulse driving for two transmons, making possible a universal quantum computation.

Acknowledgments

I would like to thank my tutor, Dr. Bruno Juliá; Dr. Maria Aranzazu Fraile Rodriguez for giving me extra material on superconduction; my external supervisors, Albert Solana and Marta P. Estarellas, and of course, the person who guided me through the process, Christian Hensel, for his daily support and patience.

[1] F. Arute, K. Arya, R. Babbush, D. Bacon, J. C. Bardin, R. Barends, R. Biswas, S. Boixo, F. G. Brandao, D. A. Buell, and et al., "Quantum supremacy using a programmable superconducting processor," *Nature*, vol. 574, p. 505–510, Oct 2019.

[2] J. G. R. Juan, *Quantum Information and quantum optics with superconducting circuits*. Cambridge University Press, 2022.

[3] Y.-x. Liu, J. Q. You, L. F. Wei, C. P. Sun, and F. Nori, "Optical selection rules and phase-dependent adiabatic state control in a superconducting quantum circuit," *Phys. Rev. Lett.*, vol. 95, p. 087001, Aug 2005.

[4] J. Q. You and F. Nori, "Atomic physics and quantum optics using superconducting circuits," *Nature*, vol. 474, p. 589–597, Jun 2011.

[5] J. Koch, T. M. Yu, J. Gambetta, A. A. Houck, D. I. Schuster, J. Majer, A. Blais, M. H. Devoret, S. M. Girvin, and R. J. Schoelkopf, "Charge-insensitive qubit design derived from the cooper pair box," *Phys. Rev. A*, vol. 76, p. 042319, Oct 2007.

[6] D. J. Griffiths and D. F. Schroeter, *2.3 The harmonic oscillator*, p. 39–54. Cambridge University Press, 3rd ed., 2018.

[7] R. Combescot, *Superconductivity: An Introduction*. Cambridge University Press, 2022.

[8] D. T. Tran, C.-W. Tai, G. Svensson, and E. Olsson, "Atomic structure and oxygen deficiency of the ultrathin aluminium oxide barrier in Al/AlOx/Al josephson junctions," *Nature News*, Jul 2016.

[9] F. K. Wilhelm, "Superconducting quantum bits," *Nature News*, Jun 2008.

[10] V. Bouchiat, D. Vion, P. Joyez, D. Esteve, and M. H. Devoret, "Quantum coherence with a single cooper pair," *Physica Scripta*, vol. 1998, p. 165, jan 1998.

[11] A. Cottet, *Implementation of a quantum bit in a superconducting circuit*. PhD thesis, Universite Paris VI, 2002.

[12] QiskitTextbook, "Introduction to transmon physics." `https://learn.qiskit.org/course/quantum-hardware-pulses/introduction-to-transmon-physics`. (2023, May 21).

[13] Numpy, "Numpy eigh function documentation." `https://numpy.org/doc/stable/reference/generated/numpy.linalg.eigh.html`. (2023, May 11).